

## Multi-mode inversion of multi-channel analysis of surface waves (MASW) dispersion curves and high-resolution linear radon transform (HRLRT)

Julian Ivanov,\* Richard D. Miller, Jianghai Xia, and Shelby Peterie, Kansas Geological Survey, The University of Kansas

### Summary

We analyze seismic data using multi-channel analysis of surface waves (MASW) to invert multi-mode surface-wave dispersion curves into 1D vertical shear-wave velocity profiles. The dispersion-curve patterns of the Rayleigh wave are imaged using conventional methods and the high-resolution linear radon transform (HRLRT). Comparison of these imaging techniques shows that the HRLRT provides higher imaging resolution of the dispersion-curve pattern that can be critical for observing and interpreting fundamental- and higher-mode dispersion-curve events of surface-wave energy. The authors conclude that multi-mode dispersion-curve inversion needs to be paired with HRLRT for the correct identification and estimation of fundamental- and higher-mode dispersion-curve data to arrive at accurate inversion results.

### Introduction

Surface waves can be observed on seismic data and used for the estimation of shear-wave velocity ( $V_s$ ), which is important for the evaluation of the stiffness properties of the near-surface materials;  $V_s$  increases as material shear strength (rigidity) increases. We use the multichannel analysis of surface wave (MASW) method to estimate near-surface shear-wave velocity from high-frequency ( $\geq 2$  Hz) Rayleigh-wave data (Miller et al., 1999a; Song et al., 1989; Park et al., 1999; Xia et al., 1999a). Shear-wave velocities estimated using MASW have reliably and consistently correlated with drill data. Using the MASW method, Xia et al. (2000) noninvasively measured  $V_s$  within 15% of  $V_s$  measured in wells. Miller et al. (1999) mapped bedrock with 0.3-m (1-ft) accuracy at depths of about 4.5-9 m (15-30 ft), as confirmed by numerous borings. The MASW method has been applied to problems such as characterization of pavements (Ryden et al., 2004), the study of Poisson's ratio (Ivanov et al., 2000), study of levees and subgrade (Ivanov et al., 2005; Ivanov et al., 2006c), investigation of sea-bottom sediment stiffness (Ivanov et al., 2000; Kaufman et al., 2005; Park et al., 2005), mapping of fault zones (Ivanov et al., 2006a), detection of dissolution features (Miller et al., 1999b), and measurement of S-wave velocity as a function of depth (Xia et al., 1999b). Studies on the MASW method have been extended to areas of determination of near-surface Q (Xia et al., 2002), and the acquisition of more realistic seismic refraction models (Ivanov et al., 2006b; Ivanov et al., 2007).

The MASW method is applied by performing the following steps. A single seismic-data record is acquired by a set of low-frequency (e.g., 4.5 Hz) geophones evenly spaced along a line. The seismic data from such a shot record is transformed into a phase-velocity – frequency domain image (i.e., dispersion-curve image), which is used to evaluate the dispersion-curve trend of the fundamental-mode of the Rayleigh wave. The estimated dispersion curve is then inverted to produce a 1-D  $V_s$  model (Xia et al., 1999a), which is assigned to the middle of the geophone spread. By assembling numerous 1-D  $V_s$  models derived from consecutively recorded seismic shot records along a seismic line, a 2-D  $V_s$  model can be obtained.

Most recent developments of the MASW method include the expansion of the conventional multichannel dispersion-curve imaging techniques (McMechan et al., 1981; Song et al., 1989; Park et al., 1998; Xia et al., 2007) with the development of the high-resolution linear radon transform (HRLRT) (Luo et al., 2008). It was reported that the HRLRT can increase image resolution by more than 100% and that higher modes can be easily distinguished. As well, the traditional fundamental-mode dispersion-curve inversion has been expanded with the inclusion and inversion of higher modes (Xia et al., 2003; Beaty et al., 2002; Beaty and Schmitt, 2003; Luo et al., 2007). It was reported that the addition of first and second higher-mode dispersion curves reduced the relative error of inversion results (compared to borehole data) to 3.6% in comparison to 15% when only the fundamental mode dispersion-curve data was used for the inversion process.

Encouraged by the reduced error results, we tested multimode inversion on various data sets and noticed that at some sites multimode dispersion-curve inversion performs poorly by converging to a relatively large root-mean-square (RMS) error and providing poor fit between some parts or all of the observed and calculated dispersion-curve data. Further study of the inversion process, from one iteration to another, showed how changes in velocity for a given layer would improve the fit for one mode and worsen for another.

In efforts to resolve such problems we used the HRLRT dispersion-curve imaging algorithm to estimate dispersion-curve data. The new images revealed that at such sites conventional algorithms (e.g., Park et al., 1998) failed to separate different modes within given frequency ranges, making them appear as one mode. Using the HRLRT dispersion-curve images to reinterpret and estimate different

## Multi-mode MASW and HRLRT

dispersion-curve modes we successfully inverted the new dispersion-curve data, which provided a good fit between the calculated and measured dispersion-curve data and converged to an acceptably low RMS error.

### Data Acquisition

Seismic data were collected in the Sonora Desert, Arizona, using a 96-channel Geometric Geode distributed seismic recording system, 4.5-Hz pressure-coupled geophones spaced every 1 m, and a hydraulic actuated, spring accelerated weight drop. Geological information suggests that the first 100 m of sediment are composed predominantly of silt, gravel, and sand (Figure 1). Seismic data were acquired at four source offsets of 1, 9, 19, and 29 m.



Figure 1. Sonora Desert, Arizona, seismic data collection site.

### Results

For each source offset we used eight spread-size ranges of 15, 25, 35, 45, 55, 65, 75, and 95 m that were transformed into phase-velocity – frequency domain images using a conventional algorithm (Park et al., 1998) with the goal of finding out which of the 32 source-spread size combinations provides the best quality fundamental-mode dispersion-curve trend in terms of resolution and widest frequency range observation (Ivanov et al., 2008). The receiver spread that was 45 m wide with the source located 1 m from the nearest receiver provided the best fundamental-mode dispersion curve image in a wide frequency range of 12-72 Hz at a velocity range of 400-300 m/s (Figure 2).

The dispersion-curve trends of 27-75 Hz at 650-500 m/s and 35-75 Hz at 1100-600 m/s were interpreted and estimated as the first and second higher modes. The fundamental, the first, and the second higher-mode data were then jointly inverted into a 1D  $V_s$  profile (Figure 3).

It can be noticed that above 40 Hz the calculated values of the fundamental mode (~400 m/s) are greater than the measured data and the calculated values of the first higher

mode (~500-550 m/s) are lower than measured data. Studying layer velocity changes from one iteration to the next during the inversion process showed that any changes in velocity for a given layer would improve the fit for one mode and worsen it for another. That explained why it was not possible to obtain a small RMS error and a good fit between the calculated and measured dispersion-curve data.

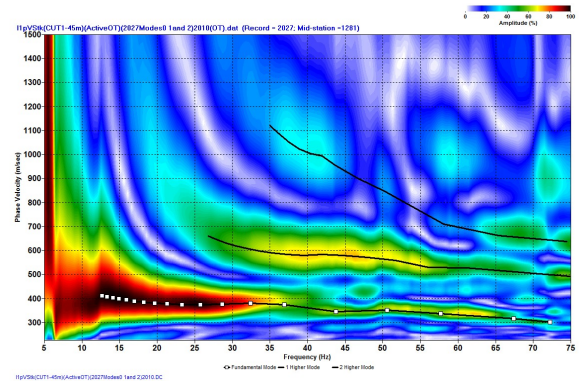


Figure 2. Conventional dispersion-curve image of MASW seismic data acquired near Yuma, Arizona. Thick black line with white squares trend is interpreted as fundamental mode. Thick black lines at higher velocities are interpreted as first and second higher modes.

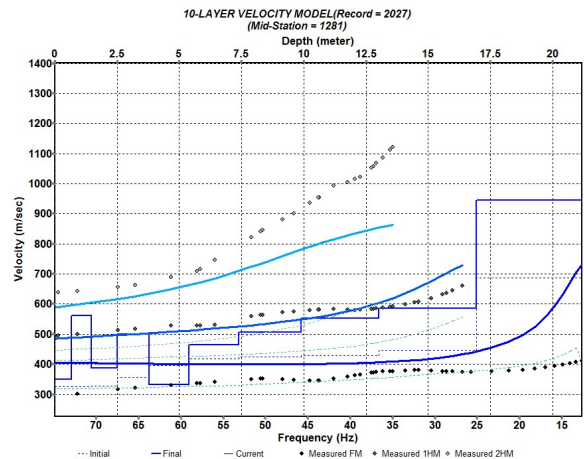


Figure 3. Multimode MASW inversion showing the fundamental, first, and second higher-mode dispersion-curve data interpreted from a dispersion curve-image obtained with a conventional imaging method. Dots indicate measured and thick lines indicate calculated dispersion-curve data. The lighter the color, the higher the mode.

In efforts to provide a better fit between the calculated and measured dispersion-curve data we researched the possibility of varying model parameters usually assumed constant during

## Multi-mode MASW and HRLRT

the inversion process, such as compressional-wave velocity ( $V_p$ ) and density. Based on the work of Xia et al., (1999a), who showed that a 25% increase in  $V_p$  resulted in less than 3% change in the final  $V_s$  values, we needed to significantly change the  $V_p$  values of the initial model to see any impact on the solution. The  $V_p$  values were changed to the extent that notably unrealistic  $V_p/V_s$  ratio initial-model values resulted, just for the purpose of finding a better numerical fit. Still, even making such extreme and unrealistic numerical assumptions, it was not possible to find an acceptable fit between the calculated and measured dispersion-curve data.

In a similar manner, we tested the inversion with varying density values based on the study of Ivanov et al. (2009), which showed that increasing density variation with depth can reduce the final inverted  $V_s$  results typically by 6-7% for the most of the middle layers from the velocity model and as much as 15% for some individual layers. Furthermore, density variations were combined with  $V_p$  variations, so a significant number of initial model combinations and final  $V_s$  results were tested. Additional inversion tests were performed trying to find other inversion parameters (e.g., number of layers, initial model, depth conversion ratio) that would improve the inversion. Still, it wasn't possible to find an acceptable fit between the calculated and measured dispersion-curve data.

Next, our quest for finding a better solution for this data was expanded using the HRLRT for dispersion-curve imaging (Figure 4). As expected from previous work (Luo et al., 2008), the main dispersion-curve events can be observed with higher resolution. Moreover, in comparison with the conven-

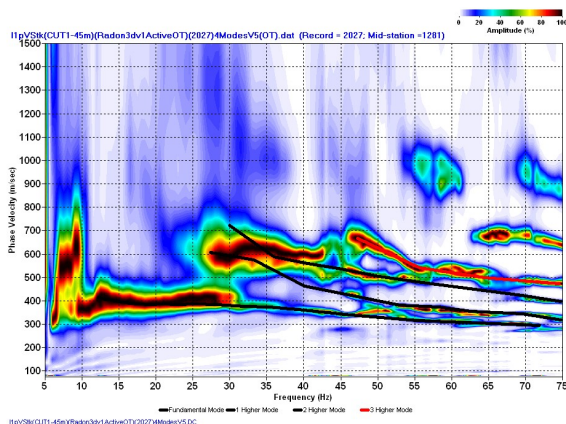


**Figure 4.** HRLRT dispersion-curve image of MASW seismic data acquired near Yuma, Arizona. Thick black lines are interpreted as fundamental mode at the lowest velocity and the second and third higher modes as higher velocities, respectively. Thick red line at the highest velocities is interpreted as the fourth higher mode.

tional method (i.e., Park et al., 1998) the HRLRT transform is able to separate different dispersion-curve events that appear as one event on the conventional method image. The fundamental mode and at least five more higher modes can be interpreted on the HRLRT image. Dispersion-curve events were reinterpreted and estimated again. We picked the same dispersion-curve events for consistency and that required the use of an additional third higher mode. Note that the event interpreted as the first higher mode on the conventional image was reinterpreted on the HRLRT image as three different higher modes (first, second, and third).

The inversion of the newly estimated multimode dispersion-curve data set quickly converged to an excellent fit between the calculated and measured dispersion-curve data (Figure 5).

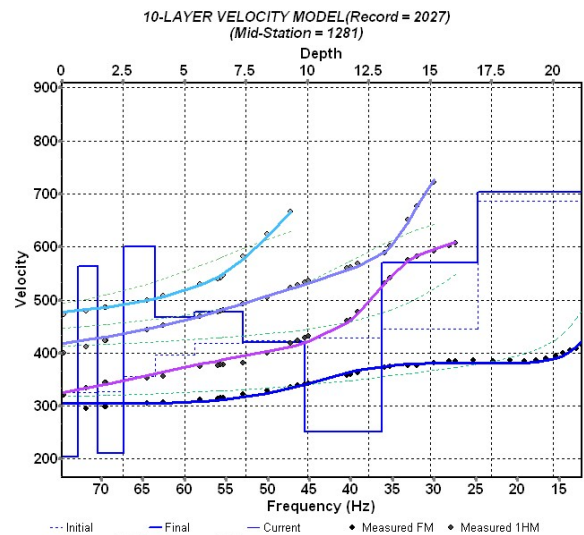


**Figure 5.** Multimode MASW inversion showing the fundamental, the first, second and the third higher mode dispersion-curve data interpreted from a dispersion curve-image obtained with the HRLRT method. Dots indicate measured and thick lines indicate calculated dispersion-curve data. The lighter the color the higher the mode.

## Conclusions

Accurate inversion of multimode dispersion-curve data is possible only after proper interpretation and identification of dispersion-curve events.

Observation of a difficultly converging multimode inversion process can be used as an indication of inadequate mode interpretation.

## Multi-mode MASW and HRLRT

It was demonstrated that the HRLRT imaging method provides not only better resolution but also allows better interpretation of dispersion-curve events, especially higher modes.

These imaging and inversion results indicate that it might be very helpful if multimode inversion is used in conjunction with the HRLRT dispersion-curve imaging method for accurate identification and estimation of dispersion-curve events, especially higher modes.

### Acknowledgments

We appreciate Mary Brohammer's assistance in manuscript preparation. The authors would like to acknowledge field assistance by Brett C. Bennett, Brett Wedel, Tony Wedel, and Justin Schwarzer during data acquisition.



**EDITED REFERENCES**

Note: This reference list is a copy-edited version of the reference list submitted by the author. Reference lists for the 2010 SEG Technical Program Expanded Abstracts have been copy edited so that references provided with the online metadata for each paper will achieve a high degree of linking to cited sources that appear on the Web.

**REFERENCES**

- Beatty, K. S., and D. R. Schmitt, 2003, Repeatability of multimode Rayleigh-wave dispersion studies: *Geophysics*, **68**, 782–790, [doi:10.1190/1.1581031](https://doi.org/10.1190/1.1581031).
- Beatty, K. S., D. R. Schmitt, and M. Sacchi, 2002, Simulated annealing inversion of multimode Rayleigh wave dispersion curves for geological structure: *Geophysical Journal International*, **151**, no. 2, 622–631, [doi:10.1046/j.1365-246X.2002.01809.x](https://doi.org/10.1046/j.1365-246X.2002.01809.x).
- Ivanov, J., R. D. Miller, and G. Tsoflias, 2009, Practical aspects of MASW inversion using varying density: *Symposium on the Application of Geophysics to Engineering and Environmental Problems*, **22**, 171–177.
- Ivanov, J., R. D. Miller, and G. Tsoflias, 2008, Some practical aspects of MASW analysis and processing: *Symposium on the Application of Geophysics to Engineering and Environmental Problems*, **21**, No. 1, 1186–1198.
- Ivanov, J., R. D. Miller, and J. Xia, 2007, Applications of the JARS method to study levee sites in southern Texas and southern New Mexico: *77th Annual International Meeting, SEG, Expanded Abstracts*, 1725–1729.
- Ivanov, J., R. D. Miller, P. J. Lacombe, C. D. Johnson, and J. W. Lane Jr., 2006a, Delineating a shallow fault zone and dipping bedrock strata using multichannel analysis of surface waves with a land streamer: *Geophysics*, **71**, no. 5, A39–A42. [doi:10.1190/1.2227521](https://doi.org/10.1190/1.2227521)
- Ivanov, J., R. D. Miller, J. Xia, D. Steeples, and C. B. Park, 2006b, Joint analysis of refractions with surface waves—An inverse solution to the refraction-travel-time problem: *Geophysics*, **71**, no. 6, R131–R138, [doi:10.1190/1.2360226](https://doi.org/10.1190/1.2360226).
- Ivanov, J., and R. D. Miller, N. Stimac R. F. Ballard J.B. Dunbar, and S. Smullen, 2006c, Time-lapse seismic study of levees in southern Texas: *76th Annual International Meeting, SEG, Expanded Abstracts*, 3255–3258.
- Ivanov, J., R. D. Miller, J. B. Dunbar, and S. Smullen, 2005, Time-lapse seismic study of levees in southern Texas: *75th Annual International Meeting, SEG, Expanded Abstracts*, 1121–1124.
- Ivanov, J. M., C. B. Park, R. D. Miller, and J. Xia, 2000, Mapping Poisson's ratio of unconsolidated materials from a joint analysis of surface-wave and refraction events: *Proceedings of the Symposium on the Application of Geophysics to Engineering and Environmental Problems*
- Kaufmann, R. D., J. Xia, R. Benson, L. B. Yuhr, D. W. Casto, and C. B. Park, 2005, Evaluation of MASW data acquired with a hydrophone streamer in a shallow marine environment: *Journal of Environmental & Engineering Geophysics*, **10**, no. 2, 87–98, [doi:10.2113/JEEG10.2.87](https://doi.org/10.2113/JEEG10.2.87).
- Luo, Y., J. Xia, R. J. Liu, Q. Liu, and S. Xu, 2007, Luo, Y., J. Xia, J. Liu, Q. Liu, and S. Xu, 2007, Joint inversion of high-frequency surface waves with fundamental and higher modes: *Journal of Applied Geophysics*, **62**, no. 4, 375–384, [doi:10.1016/j.jappgeo.2007.02.004](https://doi.org/10.1016/j.jappgeo.2007.02.004).
- McMechan, G. A., and M. J. Yedlin, 1981, Analysis of dispersive waves by wave field transformation: *Geophysics*, **46**, 869–874, [doi:10.1190/1.1441225](https://doi.org/10.1190/1.1441225).

- Miller, R. D., J. Xia, C. B. Park, and J. M. Ivanov, 1999a, Multichannel analysis of surface waves to map bedrock: *The Leading Edge*, **18**, no. 12, 1392–1396, [doi:10.1190/1.1438226](https://doi.org/10.1190/1.1438226).
- Miller, R. D., J. Xia, C. B. Park, J. Davis, W. Shefchik, and L. Moore, 1999b, Seismic techniques to delineate dissolution features in the upper 1000 ft at a power plant: Technical Program with Biographies, 69th Annual Meeting, SEG, 492-495.
- Park, C. B., R. D. Miller, J. Xia, J. Ivanov, G. V. Sonnichsen, J. A. Hunter, R. L. Good, R. A. Burns, and H. Christian, 2005, Underwater MASW to evaluate stiffness of water-bottom sediments: *The Leading Edge*, **24**, no. 7, 724–728, [doi:10.1190/1.1993267](https://doi.org/10.1190/1.1993267).
- Park, C. B., R. D. Miller, and J. Xia, 1999, Multichannel analysis of surface waves: *Geophysics*, **64**, no. 3, 800–808, [doi:10.1190/1.1444590](https://doi.org/10.1190/1.1444590).
- Park, C. B., R. D. Miller, and J. Xia, 1998, Imaging dispersion curves of surface waves on multi-channel record: 68th Annual International Meeting, SEG, Expanded Abstracts, 1377-1380
- Ryden, N., C. B. Park, P. Ulriksen, and R. D. Miller, 2004, Multimodal approach to seismic pavement testing: *Journal of Geotechnical and Geoenvironmental Engineering*, **130**, no. 6, 636–645, [doi:10.1061/\(ASCE\)1090-0241\(2004\)130:6\(636\)](https://doi.org/10.1061/(ASCE)1090-0241(2004)130:6(636)).
- Song, Y. Y., J. P. Castagna, R. A. Black, and R. W. Knapp, 1989, Sensitivity of near-surface shear-wave velocity determination from Rayleigh and Love waves: 59th Annual International Meeting, SEG, Expanded Abstracts, 509–512.
- Xia, J., Y. Xu, and R. D. Miller, 2007, Generating image of dispersive energy by frequency decomposition and slant stacking: *Pure and Applied Geophysics*, **164**, no. 5, 941–956, [doi:10.1007/s00024-007-0204-9](https://doi.org/10.1007/s00024-007-0204-9).
- Xia, J., R. D. Miller, C. B. Park, and G. Tian, 2003, Inversion of high frequency surface waves with fundamental and higher modes: *Journal of Applied Geophysics*, **52**, no. 1, 45–57, [doi:10.1016/S0926-9851\(02\)00239-2](https://doi.org/10.1016/S0926-9851(02)00239-2).
- Xia, J., R. D. Miller, C. B. Park, and G. Tian, 2002, Determining Q of near-surface materials from Rayleigh waves: *Journal of Applied Geophysics*, **51**, no. 2-4, 121–129, [doi:10.1016/S0926-9851\(02\)00228-8](https://doi.org/10.1016/S0926-9851(02)00228-8).
- Xia, J., R. D. Miller, C. B. Park, J. A. Hunter, and J. B. Harris, 2000, Comparing shear-wave velocity profiles from MASW with borehole measurements in unconsolidated sediments, Fraser River Delta, B.C., Canada: *Journal of Environmental & Engineering Geophysics*, **5**, no. 3, 1–13, [doi:10.4133/JEEG5.3.1](https://doi.org/10.4133/JEEG5.3.1).
- Xia, J., R. D. Miller, and C. B. Park, 1999a, Estimation of near-surface shear-wave velocity by inversion of Rayleigh waves: *Geophysics*, **64**, 691–700, [doi:10.1190/1.1444578](https://doi.org/10.1190/1.1444578).
- Xia, J., R. D. Miller, C. B. Park, J. A. Hunter, and J. B. Harris, 1999b, Evaluation of the MASW technique in unconsolidated sediments: 69th Annual International Meeting, SEG, Expanded Abstracts, 437-440.